Green Sciences
Volume 28 Issue 1 · pp. 44–59 · DOI: 10.2478/pjct-2026-0004

Integrated biovalorization of *Pongamia pinnata* seeds for sustainable biodiesel and bioethanol production

Research Article

Sidra Rani[1], Zahid Anwar[1]*, Zafar Iqbal[2]*, Muddassar Zafar[1], Hafiz Muhammad Javed[1]

[1] *Department of Biochemistry and Biotechnology, University of Gujrat, Gujrat, 50700, Pakistan*
[2] *Central Laboratories, King Faisal University, Al-Ahsa, P.O. Box 31982, Saudi Arabia*

Received 26 October 2025; Accepted 08 February 2026

Abstract: Biofuels represent a sustainable alternative to fossil fuels, with non-food feedstock offering particular promise. This study evaluated *Pongamia pinnata* seeds as a dual feedstock for biodiesel and bioethanol production. Moisture content was determined at 8.0%, favorably lower than most lignocellulosic biomasses. FTIR analysis confirmed the presence of cellulose, hemicellulose, and lignin, indicating its suitability for biofuel production. Biodiesel was produced via alkaline transesterification, with the highest conversion (70%) obtained at a 5:1 alcohol-to-oil ratio. The de-oiled seed cake, rich in carbohydrates and low in lignin, was optimized for glucose release through Response Surface Methodology. Optimal conditions (100°C, 2.5 g substrate, 1.75% H_2SO_4, 60 min) yielded 429 mg g^{-1} glucose. Enzymatic hydrolysis further enhanced sugar release, with maximum glucose (118.21 mg g^{-1}) achieved at 72 h with a 2.0 mL enzyme load. Subsequent fermentation with *Saccharomyces cerevisiae* produced 6.71% ethanol. These findings highlight the potential of *P. pinnata* as a feedstock for integrated biorefineries, supporting sustainable biofuel production.

Keywords: *Bioethanol* • *Biodiesel* • *Biomass* • *FTIR* • Pongamia pinnata • *Valorization*

Abbreviations

The following abbreviations are used in this manuscript:

FTIR	Fourier Transform Infrared Spectroscopy
Pongamia pinnata	*P. pinnata*
RSM	Response Surface Methodology
Saccharomyces cerevisiae	*S. cerevisiae*

1. Introduction

The escalating global energy demand, coupled with the dwindling reserves of fossil fuels and their detrimental environmental impact, necessitates the exploration of sustainable and renewable energy alternatives [1]. Intensified agricultural practices aimed at meeting growing food needs generate substantial agro-cellulosic biomass, posing a significant environmental challenge due to inefficient disposal and mismanagement [2]. Global biomass waste generation is estimated at 140 gigatons per annum, with severe environmental consequences. Biofuels, derived from renewable biological sources, have emerged as promising contenders to mitigate our reliance on fossil fuels and contribute to a more sustainable energy future [3]. Among various feedstocks, non-edible oilseed plants offer a compelling alternative to food crops, minimizing the competition for land and resources [4].

Lignocellulosic biomass, the most abundant renewable resource, presents a significant challenge for bioethanol production due to its complex structure comprising 30–50% cellulose, 15–30% hemicellulose, and 15–30% lignin by dry weight [5]. This complex structure comprises cellulose (30–50% of dry weight), hemicellulose (15–30%), and lignin (15–30%) [5], Lignin, in particular, hinders the

* *E-mail: Zahid.anwar@uog.edu.pk, zafar@kfu.edu.sa*

Open Access. © 2026 Sidra Rani *et al.*, published by West Pomeranian University of Technology, Szczecin
This work is licensed under the Creative Commons Attribution-NonCommercial-NoDerivs 4.0 License.

enzymatic hydrolysis of cellulose and hemicellulose into fermentable sugars. Pretreatment is crucial to overcome this barrier, but it often increases the overall production cost [6]. Dilute acid pretreatment at elevated temperatures effectively disrupts the lignocellulosic structure, promoting hemicellulose hydrolysis and enhancing subsequent enzymatic hydrolysis of cellulose [7]. To optimize pretreatment conditions and minimize costs, Response Surface Methodology (RSM) with Central Composite Design (CCD) can be employed. RSM utilizes statistical analysis to identify optimal conditions for specific process variables (e.g., acid concentration, temperature, reaction time, substrate amount), thereby minimizing resource usage and maximizing process efficiency.

Pongamia pinnata (L.) (common name Sukh chain/ Indian beach tree; family *Fabaceae*), also known as *Derris indica*, is a monotypic, fast-growing, drought-tolerant tree. It is native to tropical and subtropical regions of India, Pakistan, and Southeast Asia. It thrives in diverse environments and has been successfully cultivated worldwide, including China, Australia, New Zealand, and the USA. *P. pinnata* is a rich source of various phytochemicals. Its seeds contain a diverse array of compounds, including six composites (two sterols, three sterol derivatives, and one double sugar) and 8 fatty acids (three saturated and five unsaturated), including linoleic acid, oleic acid, stearic acid, behenic acid, α-linolenic acid, lignoceric acid, and eicosenoic acid [8]. Isolated compounds from *P. pinnata* seeds include karangin, pongagalabrone, pongapin, pinnatin, and kanjone [9]. The cultivation of *P. pinnata* in the Indo-Pak region offers numerous ecological and economic benefits. Its ability to fix atmospheric nitrogen enhances soil fertility, making it an ideal choice for agroforestry systems. Moreover, the tree's tolerance to marginal lands ensures its utility in areas unsuitable for conventional crops. Despite the availability of approximately 200 million tons of *P. pinnata* seeds in this region, only 6% of this potential is currently exploited, highlighting the need for optimized utilization strategies [10].

P. pinnata is a non-edible oil-yielding tree with high potential for seed yield (~20,000 seeds/tree) [11] and has unprecedented potential as a biofuel feedstock due to its high oil content (28–39% in seeds), rich in polyunsaturated fatty acids [12,13]. In India, it is among the best sources for biodiesel production, yielding 0.055 metric tonnes of vegetable oil per plant. The oilcake and starch from *P. pinnata* seeds can be efficiently utilized for bioethanol production [14]. As non-edible seeds, they are suitable for biofuel applications without competing with food crops [15,16]. Its seeds are rich in oil, making them suitable for biodiesel production, while the residual biomass can be further utilized for bioethanol production [17]. So, *P. pinnata* offers several advantages as a biofuel feedstock: adaptability to diverse environments, high oil content with a favorable fatty acid profile for biodiesel, and the potential for bioethanol production from residual lignocellulosic biomass [15,16].

Building on these advantages, this study develops and optimizes an integrated biorefinery process for sustainable biofuel production from *P. pinnata* seeds by strategically coupling biodiesel and bioethanol production pathways. A key novelty lies in evaluating direct base-catalyzed transesterification of high-free fatty acid crude oil under optimized conditions, demonstrating the feasibility of a simplified process without acid pretreatment. Biodiesel production is further integrated with physicochemical characterization and valorization of the residual lignocellulosic fraction, enabling holistic biomass utilization. Collectively, the achieved conversion efficiencies, fuel properties, and residue characteristics highlight improved resource utilization, reduced waste generation, and enhanced process efficiency, thereby strengthening the economic and environmental viability of *P. pinnata*-based biorefineries for sustainable biofuel production.

2. Materials and methods

2.1 Biomass Collection and determination of moisture contents

Non-edible seeds of *P. pinnata* were collected from the vicinity of the University of Gujrat, Gujrat, Pakistan (32°38′26″N; 74°10′01″E). The collected biomass was thoroughly washed with distilled water to remove surface contaminants and then dried under sunlight for 48 h (h). Subsequently, the dried biomass was ground into a fine powder with a uniform particle size ranging from 20 to 40 mesh. The ground biomass was then stored in an airtight plastic jar for further use.

The moisture content of *P. pinnata* seeds was determined using the standard oven drying method. Precisely weighed *P. pinnata* seeds (1.0 g) were placed in pre-dried and tared aluminum dishes and dried to constant weight in a laboratory oven set at 60–65°C. The moisture content, expressed as a percentage, was calculated from the difference between the initial and final dry weights, using the formula given below, as described earlier [18,19].

$$MC = \frac{\text{Initial weight (mm)} - \text{Ovendry weight (mm)}}{\text{Initial weight (mm)}} \times 100$$

2.2 Chemical analysis through Fourier-transform infrared spectroscopy

A Fourier-transform infrared spectrophotometer (FTIR; IR Affinity-1, Shimadzu, Kyoto, Japan) was employed to characterize the functional groups present in *P. pinnata* seeds. Finely ground *P. pinnata* seed powder was thoroughly mixed with spectroscopic grade potassium bromide (KBr) at a ratio of approximately 1:100 (w/w) and pressed into translucent pellets of 1 mm thickness using a hydraulic press under vacuum. FTIR spectra were recorded in the range of 4,000–650 cm^{-1} with a spectral resolution of 4 cm^{-1}, ensuring high accuracy and reproducibility, as described earlier [20].

2.3 Oil extraction

Oil from *P. pinnata* seeds was extracted by the solvent extraction method [21]. The extraction solvent, a mixture of *n*-hexane and isopropanol in a 3:2 (v/v) ratio, was prepared by mixing hexane (300 mL) and isopropanol (200 mL). This specific solvent system was chosen for its effectiveness in extracting a broad spectrum of lipids and ensuring high oil recovery. One gram of ground *P. pinnata* seeds was mixed with 50 mL of the solvent mixture in a conical flask. The flask was incubated in a temperature-controlled shaking water bath (model WBC-22,Wincom) at 50°C and 150 rpm for 30 min. The resulting mixture was filtered through filter paper (Whatman no. 1). To ensure complete oil recovery, the solid residue on the filter paper was washed with an additional 10 mL of pre-warmed solvent. The combined filtrates were then subjected to rotary evaporation (Heidolph, Hei-VAP value) at 70°C and 0.07 atm vacuum pressure to remove the solvent. The extracted oil was collected but not subjected to detailed analytical characterization (e.g., acid value, viscosity), but relied on established literature values for *P. pinnata* oil properties. The weight and volume of the extracted oil were measured to calculate the oil yield (%), with the following formula.

$$\text{Percent yield} = \frac{\text{amount of recovered oil (g)}}{\text{amount of sample used (g)}} \times 100$$

Notably, the physicochemical properties and fatty acid composition of *P. pinnata* oil, including free fatty acid content, were adopted from well-established literature reports and used as reference values for process optimization [8,9].

2.4 Transesterification of the oil

As *P. pinnata* oil contained significantly high free fatty acid (FFA) content (~18%) [22], a two-step transesterification process was followed to ensure efficient biodiesel conversion. Initially, acid pre-esterification was performed to reduce FFA content to a level suitable for subsequent alkaline transesterification. The reaction mixture was carried out in a 250-mL conical flask containing the oil and 100 mL of a 70% (v/v) ethanol, with NaOH (0.5% w/w of oil) used as the catalyst. Ethanol-to-oil molar ratios of 2:1, 3:1, 4:1, 5:1, and 6:1 were evaluated by adjusting the volume of the 70% ethanol solution relative to the oil. The reaction mixture was maintained at 60–70°C and stirred at 750 rpm for 1–2 h to facilitate transesterification. Upon completion, the reaction mixture was cooled to room temperature and transferred to a separating funnel to isolate the distinct biodiesel layer, which formed at the top. The biodiesel was then washed multiple times with warm distilled water (50°C) until the washing water reached a neutral pH. Residual water was removed by drying the biodiesel at 100°C for 30 min in a vacuum oven. The biodiesel yield was then determined using the gravimetric method, calculating the percentage conversion based on the initial oil weight.

2.5 Bioprocessing of biodiesel

Following oil extraction, the oil was processed into biodiesel through a series of steps, including glycerin separation and transesterification.

2.6 Separation of glycerin

The extracted oil was washed with distilled water three to four times to remove impurities and residual reagents. After each washing, the mixture was centrifuged to facilitate phase separation. A distinct white layer, containing impurities, formed at the top was carefully removed with a micropipette, as it could interfere with subsequent transesterification. The denser glycerol layer formed at the bottom was kept and collected for subsequent transesterification.

2.7 Optimization of physicochemical parameters for bioethanol by RSM

RSM with a CCD was employed to optimize the physicochemical parameters for the pretreatment of *P. pinnata*

seeds to yield maximum reducing sugars. The independent variables investigated were H_2SO_4 concentration (0.5–3% v/v), substrate concentration (0.5–5.5 g), and temperature (30–100°C).

The effects of these variables and their interactions on glucose and xylose yields, as well as lignin degradation [22], were evaluated using 3D response surface plots. A quadratic regression model [23] was used to describe the relationship between the independent variables and the responses. Statistical significance was determined using ANOVA, *F*-tests, and *t*-tests at a significance level of $p \leq 0.05$. MINITAB 17 software was used for statistical analysis, including ANOVA and the calculation of regression coefficients [24].

2.8 Acid hydrolysis and estimation of reducing sugars

De-oiled *P. pinnata* seed powder was subjected to acid hydrolysis under the RSM-optimized conditions of H_2SO_4 concentration, temperature, and time (Table 1). Twenty-five independent hydrolysis trials were performed. The resulting hydrolysates were filtered, and the solid residues were washed with distilled water. The filtrates were then used to determine the concentrations of released reducing sugars and soluble lignin using the anthrone method [25]. For the estimation of reducing sugars in each filtrate, 1 mL of sample was added to 4 mL of anthrone reagent, which was prepared by dissolving 2 g of anthrone in 1 L of 72% (v/v) H_2SO_4. The mixture was then incubated at 100°C for 8 min. After cooling to room temperature, the absorbance was measured at 540 nm using a spectrophotometer (PG80, UK). A calibration curve was generated using known concentrations of D(+)-glucose. Carbohydrate productivity (*P*), expressed as g L^{-1} day^{-1}, was calculated using the following equation:

$$P_{\text{Carbohydrate}} = \frac{c_t - c_0}{t}$$

Here, *t* is the cultivation time and c_t and c_0 are the carbohydrate concentration (g L^{-1}) at time *t* and t_0, respectively.

2.9 Enzymatic hydrolysis

The acid-pretreated substrate was washed three to four times with distilled water to neutralize residual acid. To hydrolyze the remaining polysaccharides (cellulose, hemicellulose, and starch) in de-oiled *P. pinnata* biomass, enzymatic hydrolysis was performed using a 1:1 (v/v) mixture of indigenously produced endoglucanase and exoglucanase. The highest yielding enzyme activities were mixed in different volumes (0.5, 1.0, 1.5, and 2.0 mL), and the enzyme mixture was added to Erlenmeyer flasks containing 2 g of the washed substrate suspended in 100 mL of 50 mM citrate buffer (pH: 5.0–6.0). To inhibit bacterial contamination, Augmentin was added to each flask at a concentration of 75 mg L^{-1}. The flasks were then incubated at 50°C for different time intervals (1.5, 3, 24, 48, and 72 h). Samples were withdrawn at each time point, and glucose concentrations were determined using the DNS method [26]. To inhibit bacterial contamination, approximately 75 mg of Augmentin was added to each flask. The hydrolysate with the highest glucose concentration was selected for subsequent fermentation.

2.10 Inoculum preparation, fermentation, and ethanol quantification

The inoculum was prepared by cultivating *Saccharomyces cerevisiae* (Rossmoor Food Products, Karachi, Pakistan) in Yeast Peptone Dextrose (YPD) medium. The YPD medium, containing 2% casein peptone, 2% dextrose, and 1% yeast extract [27], was aliquoted into three independent 250-mL Erlenmeyer flasks, sealed with cotton plugs and aluminum foil, and autoclaved at 121°C for 30 min at 15 psi. Each flask was inoculated with approximately 2 g of yeast and incubated at 37°C for 24 h to promote optimal growth, resulting in an inoculum of 1×10^7 cells mL^{-1}.

Fermentation was carried out using the enzymatically hydrolyzed filtrates with the optimal glucose concentration. To determine the ideal inoculum size, triplicate fermentations were initiated in 250 mL Erlenmeyer flasks containing 100 mL of the hydrolysate with inoculum volumes ranging from 1 to 5 mL. The flasks were incubated at 36°C with shaking at 120 rpm for 96 h. Samples were aseptically collected at 6, 24, 48, and 72-h intervals within a laminar airflow cabinet (Heraguard™ ECO Clean Bench, Thermo Fisher Scientific, Waltham, MA, USA) for ethanol analysis [18].

The produced bioethanol was purified by distillation using a Soxhlet apparatus and quantified using the potassium dichromate method [28,29]. Briefly, 300 µL of the ethanol sample was added to 3 mL of an acid dichromate solution (0.1 M of $Cr_2O_7^{-2}$ in 5 M of H_2SO_4). The mixture was sealed with Parafilm and incubated at room temperature for 30 min. The resulting absorbance was measured at 590 nm using a spectrophotometer.

Table 1. Experimental design for RSM

SR #	Temperature (°C)	Time (min)	Acid conc. (%)	Substrate conc. (g)	Glucose conc. (mg mL^{-1})
1	30	20	3	1	35.201
2	30	20	3	4	59.110
3	30	60	0.5	1	130.112
4	30	60	0.5	4	71.211
5	30	20	0.5	1	77.341
6	30	20	0.5	4	80.322
7	60	40	1.75	2.5	177.109
8	60	40	1.75	2.5	181.214
9	30	60	3	1	44.221
10	60	40	4.25	2.5	11.298
11	60	40	1.75	5.5	123.765
12	60	40	0.25	2.5	149.246
13	60	10	1.75	2.5	69.776
14	60	80	1.75	0.5	101.209
15	30	60	3	4	14.117
16	60	40	1.75	0.5	120.328
17	20	40	1.75	2.5	116.821
18	90	20	0.5	1	260.671
19	60	40	1.75	2.5	178.109
20	90	20	0.5	4	329.432
21	90	60	0.5	1	363.119
22	100	60	1.75	2.5	429.220
23	60	40	1.75	2.5	179.402
24	60	40	1.75	2.5	177.712
25	90	60	3	1	285.996
26	90	20	3	1	248.556
27	90	20	3	4	306.245
28	60	40	1.75	2.5	180.127
29	90	60	0.5	4	350.478
30	90	60	3	4	229.492

Source: Author's contribution.

2.11 Statistical analysis

RSM Analysis, using MINITAB software, generated contour and 3D surface plots to visualize the relationships between the independent variables and to determine optimal values for maximizing the response (presumably, reducing sugar release or bioethanol production). Analysis of variance (ANOVA) was performed to assess the statistical significance of the effects of different treatments on biomass. Correlation analysis was used to determine the relationship between sugar content in the biomass and bioethanol production.

3. Results and discussion

3.1 Moisture content estimation

The moisture content of the collected *P. pinnata* seeds was determined to be 8.0%, which falls within previously

reported ranges of 7.3% [18,30] and 9% [31,32]. In contrast, other lignocellulosic biomasses typically exhibit moisture contents ranging 10–13% [33]. The observed variation in moisture content may be attributed to factors such as varietal differences, seasonal variations, habitat differences, or sampling variations. Moisture content plays a crucial role in various biological processes, facilitating nutrient transport and supporting microbial activity, which is essential for efficient lignocellulosic biomass degradation [34]. Therefore, the relatively higher moisture content of *P. pinnata* seeds may offer advantages in terms of storage stability, reduce energy expenditure for drying, while still supporting microbial activity and subsequent biofuel production compared to other lignocellulosic substrates.

3.2 Chemical analysis by FTIR

FTIR Spectroscopy was employed to infer the presence of functional groups, vibration modes, and chemical composition in the unprocessed *P. pinnata* seeds. The spectrum (Figure 1, Table 2) showed absorption bands between 700 and 3,300 cm^{-1}, indicating a complex lignocellulosic structure.

The spectrum revealed signatures of major biopolymers. A broad absorption band at 3273.11 cm^{-1} indicated hydrogen-bonded O–H stretching vibrations, typical of the hydroxyl groups in cellulose, hemicellulose, and lignin [18]. The CH_2 (C–H) symmetric stretching vibration, characteristic of cellulose, was observed at 2920.51 and 2850.99 cm^{-1} in *P. pinnata* biomass, consistent with previously reported values of 2,914–2,918 cm^{-1} for cellulosic materials [35]. Lignin-specific bands were identified at 1624.30 cm^{-1} (aromatic C=C skeletal vibrations) and in the 1,510–1,600 cm^{-1} range [35]. The presence of carbonyl groups in esters or ketones was indicated by a C=O stretching vibration at 1708.89 cm^{-1} [36].

The band at 1405.47 cm^{-1} was assigned to deformations of aliphatic $–CH_2$, $–CH_3$, and –OH groups [37]. The C–O stretching vibration observed at 1227.37 cm^{-1} is likely associated with C=O groups present in primary alcohols and ester linkages of hemicelluloses. Similarly, the stretching vibration at 1,236 cm^{-1} has been attributed to C–O groups within the cellulosic biomass [18]. A prominent peak at 1020.53 cm^{-1} corresponds to C–O stretching in primary alcohols and cellulose, a well-documented feature in lignocellulosic biomass [18,38]. Notably, a peak at 1,029 cm^{-1} has been attributed to C–F stretching vibrations in other studies [38]. Likewise, an absorbance peak at 756.02 cm^{-1} was attributed to C–Cl bonds in the halogens. Similar findings have been demonstrated for the fortification of poplar biomass [35], *Delonix regia* pods [18], corn cobs, and rice husk biomass [38]. Slight deviations in reported wavenumbers are common and likely result from differences in biomass composition and analytical conditions. The presence of aromatic C=C skeletal vibrations at 1,624 cm^{-1} confirms the lignin content, which typically requires robust pretreatment to expose cellulosic fibers [39].

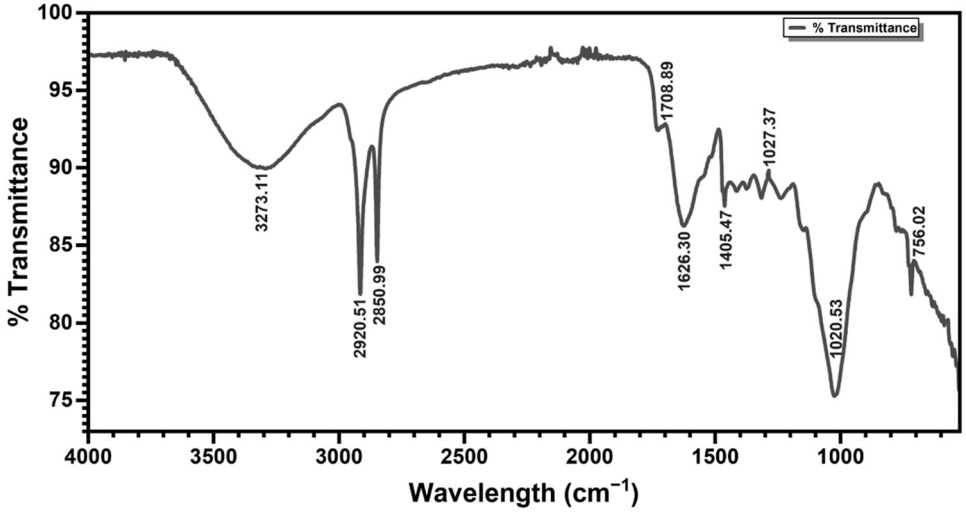


Figure 1. Fourier-transform infrared spectroscopy (FTIR) spectrum of *P. pinnata* seeds.

Source: Author's contribution.

Table 2. FTIR Spectrum of *Pongamia pinnata* seeds

Sr. #	Wave number (cm^{-1})	Functional group	Bond
1	3273.11	Alcohol	O–H
2	2920.51	Alkane	C–H
3	2850.99	Alkane	C–H
4	1708.89	Carbonyl	C–O
5	1624.30	Alkenes	C–C
6	1405.47	Phenols	–OH bending vibrations, –C–O–H in-plane bending vibrations,–CH_3 out-of-plane bending vibrations, –CH_2 – wagging and twisting vibrations
7	1227.37	Amines	N–H, C–O (hemicellulose)
8	1020.53	Halogen	C–F (guaiacyl unit of lignin) and C–O (primary alcohol and cellulose)
9	756.02	Halogen	C–Cl

Source: Author's contribution.

3.3 Biodiesel yield and process optimization

Biodiesel produced from *P. pinnata* oil and subjected to the ethanol-to-oil molar ratio optimization across a range of 2:1 to 6:1 (v/v). The alcohol-to-oil ratio exerted a pronounced effect on biodiesel yield, underscoring its critical role in transesterification efficiency.

Maximum biodiesel conversion (70%) was achieved at an ethanol-to-oil ratio of 5:1, whereas a further increase to 6:1 reduced yield to 55% (Figure 2). This decline aligns with the principle that excess alcohol can drive reverse reactions (saponification), shifting the equilibrium toward glycerol formation and reducing biodiesel yield [40]. Previous studies have reported optimal alcohol-to-oil ratios ranging from 3:1 to 10:1 depending on feedstock and reaction conditions. For example, yields of 95% and 92% have been achieved with methanol-to-oil ratios of 6:1 and 10:1, respectively [8,42], while waste cooking oil and soybean oil have yielded maximum conversions at 9:1 and 10:1 ratios [43]. Thus, careful optimization of the alcohol-to-oil ratio is essential for maximizing transesterification efficiency [44]. Mass balance analysis further corroborated these findings, corresponding to an overall conversion efficiency of 70% based on the oil content

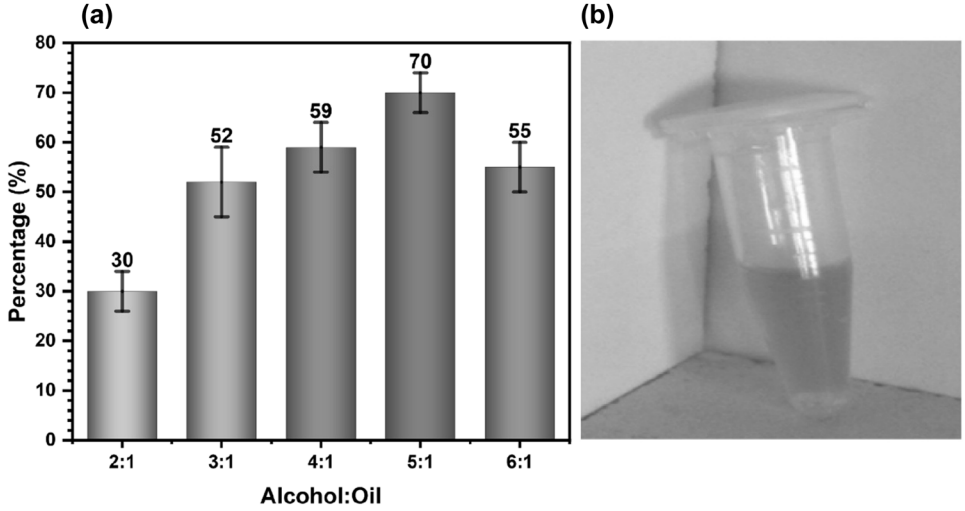


Figure 2. Alcohol to oil ratio used in the transesterification of *P. pinnata* oil (a), and Biodiesel after Washing the Oil & Transesterification Process (b). *X*-Axis represent the different alcohol to oil ratios used and SD was calculated for $n = 3$.

Source: Author's contribution.

Table 3. Coded and uncoded values of the variables for the Box–Behnken design

Sr. #	Coded values of variables	−α	−1	0	+1	+α
	Variables uncoded values					
1	Temperature (°C)	30	60	80	90	100
2	Acid concentrations (%)	0.25	0.5	1.75	53	4.25
3	Time (min)	20	30	40	60	80
4	Substrate concentrations (g)	0.5	1	2.5	4	5.5

Source: Author's contribution.

(Figure 2). This result confirms the technical feasibility of biodiesel production from *P. pinnata* oil under optimized conditions and supports its integration within a combined biodiesel–bioethanol biorefinery framework.

3.4 Optimization of physicochemical parameters by RSM

RSM Implemented in MINITAB 17 was employed to statistically optimize pretreatment conditions for de-oiled *P. pinnata* seed biomass. RSM is a widely applied statistical tool in biofuel research that reduces experimental trials while efficiently assessing the effects and interactions of variables. It has been successfully used to pretreat various lignocellulosic feedstocks, including bamboo, corn stover, corn cobs, elephant grass, sugarcane, switchgrass, wheat straw, and *Vachellia nilotica*.

Analysis of the de-oiled *P. pinnata* seed waste revealed a high content of carbohydrates (42% w/w) and a low amount of lignin, a known inhibitor of enzymatic and hydrolytic degradation [42]. This favorable composition makes it a suitable substrate for bioconversion. To optimize glucose release, an RSM design was employed using Design Expert v 7.0 software [45]. The highest glucose yield (429 mg g^{-1}) was achieved under optimal conditions of 100°C, 2.5% substrate concentration, 60 min incubation, and 1.75% H_2SO_4, with glucose quantified spectrophotometrically at 540 nm (Table 3).

3.5 Optimization of incubation time on glucose release

To visualize the interactive effects of process parameters on glucose production, contour and 3D plots were generated. These plots were created by varying substrate concentration (0.5–5.5 g), acid concentration (0.5–4.75%), and incubation time (10–80 min) while examining glucose release at both high (above 100°C) and low (30°C) temperatures. Contour and 3D plots (Figure 3a and b) indicated that maximum glucose release occurred at 55–60 min incubation with 2.5–3.0 g substrate. Shorter incubation or lower substrate concentrations resulted in reduced yields. Overall,

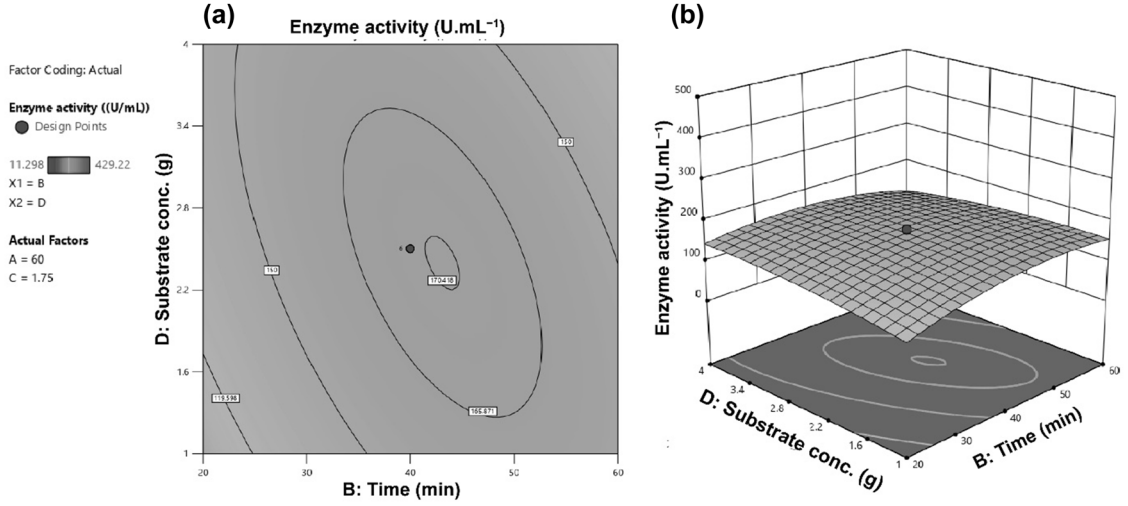


Figure 3. Contour (a) and 3D response surface plot (b) showing the interactive effects of incubation time (min) and substrate concentration (g) on glucose concentration activity during enzymatic hydrolysis of *P. pinnata* seed biomass. The red dot represents the experimental design point, while the color gradient indicates enzyme activity levels ranging from low (blue, 11.29 U mL^{-1}) to high (red, 429.22 U mL^{-1}). Actual factors were fixed at temperature = 60°C and acid concentration = 1.75%.

Source: Author's contribution.

higher temperatures and longer times improved sugar release, with 90°C, 2.5 g substrate, and 60-min incubation producing the best results. Longer incubation during biomass pretreatment enhances glucose yield by progressively disrupting the lignocellulosic matrix, thereby increasing cellulose accessibility to acids and hydrolytic enzymes. At the molecular level, extended treatment increases surface area and porosity, reduces cellulose crystallinity, and promotes lignin and hemicellulose solubilization, collectively improving enzyme–substrate interactions. However, excessively long incubation can lead to sugar degradation, underscoring the need for careful process optimization [46].

3.6 Optimization of incubation temperature on glucose release

Contour and 3D plots (Figure 4a and b) indicated that temperature strongly influenced glucose release, with optimal yields at 95–100°C and 1.5–1.75% H_2SO_4. While higher temperatures increased glucose yield by accelerating cell wall deconstruction, promoting hemicellulose hydrolysis, lignin softening and redistribution, and partial cellulose decrystallization and increasing cellulose accessibility. Nonetheless, excessively high temperatures also promote inhibitor formation and sugar degradation, which could hinder downstream fermentation [47,48]. Thus, maintaining an optimal temperature range is critical to balance sugar release and minimize inhibitor production.

3.7 Optimization of substrate concentration on glucose release

Substrate concentration had a marked effect on glucose release under optimized conditions. At 100°C for 1 h, 1 g of substrate yielded the maximum release, while contour and 3D plots (Figure 5a and b) indicated consistently high glucose concentrations at 97–100°C with 2.2–2.5 g of substrate. Further analysis revealed that 3.5–4 g of substrate combined with 1.5–1.75% H_2SO_4 also supported elevated glucose yields, whereas low concentrations (1–1.5 g) produced the least glucose regardless of acid level.

Increasing substrate concentration during pretreatment promotes more effective removal of lignin and hemicellulose by inducing structural swelling, increasing porosity, and reducing cellulose crystallinity, thereby improving cellulose accessibility. However, excessively high substrate loadings adversely affect subsequent hydrolysis efficiency and ethanol productivity by increasing mixture viscosity and limiting enzyme accessibility, thereby inhibiting glycolytic enzymes [49]. Conversely, moderate concentrations enhanced sugar release, with longer incubation times further improving yields. Similar trends have been reported in other lignocellulosic systems, where excessive solid loadings reduced hydrolysis efficiency, while optimal loadings (≈3%) improved ethanol yield (0.096 g g^{-1}). Thus, fine-tuning substrate concentration is critical for balancing glucose release and ethanol production efficiency.

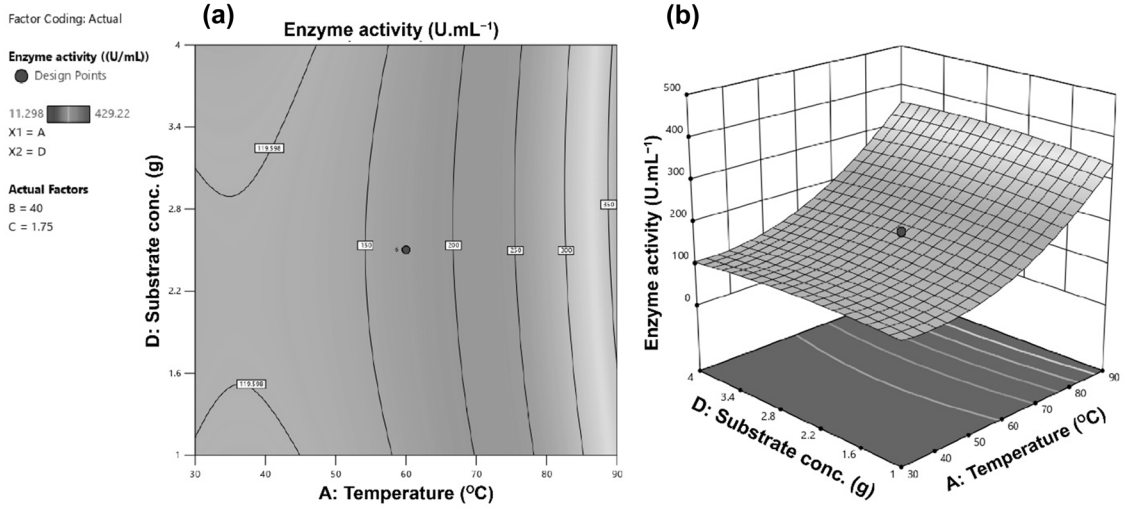


Figure 4. Contour (a) and 3D response surface plot (b) showing the interactive effects of temperature (°C) and substrate concentration (g) on glucose concentration during enzymatic hydrolysis of *P. pinnata* seed biomass. The red dot represents the experimental design point, while the color gradient indicates enzyme activity levels ranging from low (blue, 11.29 U mL^{-1}) to high (red, 429.22 U mL^{-1}). Actual factors were fixed at acid concentration = 2.5% and temperature 40°C.

Source: Author's contribution.

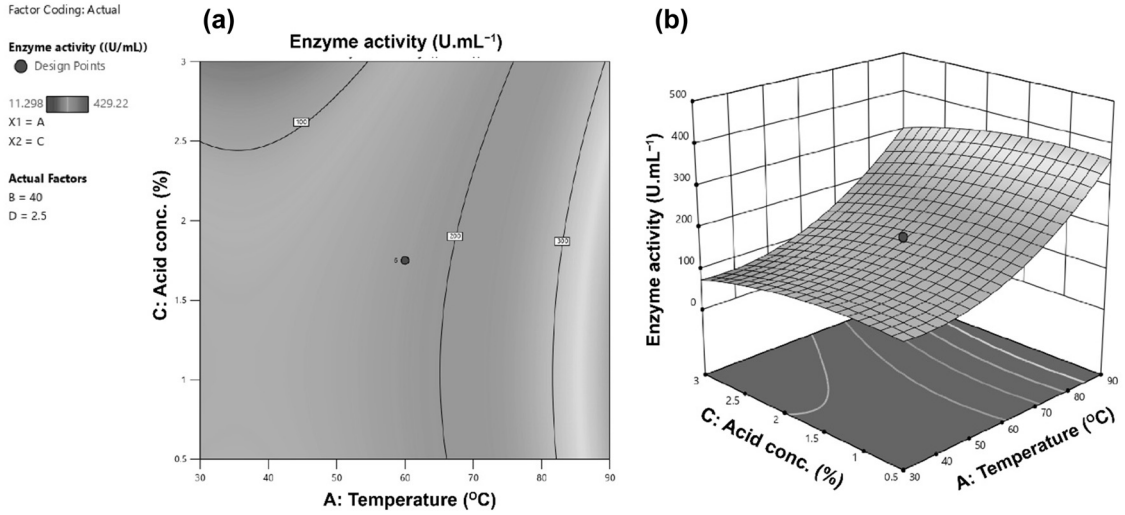


Figure 5. Contour (a) and 3D response surface plot (b) showing the interactive effects of acid concentration (%) and temperature (°C) on glucose concentration during enzymatic hydrolysis of *P. pinnata* seed biomass. The red dot represents the experimental design point, while the color gradient indicates enzyme activity levels ranging from low (blue, 11.29 U mL^{-1}) to high (red, 429.22 U mL^{-1}). Actual factors were fixed at D: acid concentration = 2.5% and B: temperature 40°C.

Source: Author's contribution.

3.8 Optimization of acid concentration and temperature on glucose release

Sulfuric acid concentration significantly influenced pretreatment, so this study used different H_2SO_4 concentrations of 0.5, 1.75, 3, and 4.25%. Strongest glucose release occurred with 1.75–2.0% H_2SO_4 combined with moderate substrate loads (1–4 g) and 60–65 min incubation. Comparisons with other biomasses (such as rice husk, corn stover) and organic and inorganic acids (such as phosphoric- and hydrochloric acid), H_2SO_4 as an effective pretreatment agent for lignocellulosic biomass. While various can be used, sulfuric acid is widely considered effective for pretreating lignocellulosic biomass that could yield a 90.8% reducing sugars from rice husk [50], 21.02% reducing sugar from *Eulaliopsis binate* [51], and 78% reducing sugar from corn stover [52].

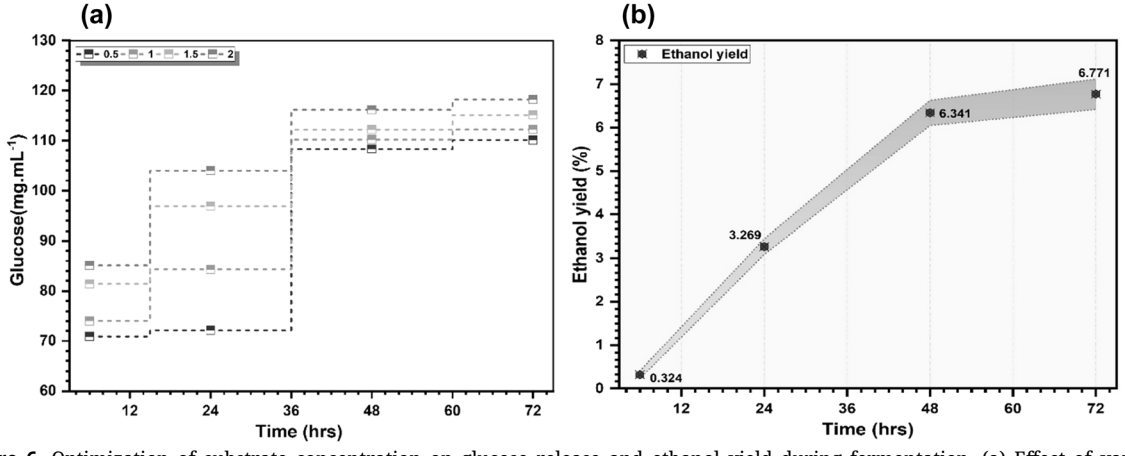


Figure 6. Optimization of substrate concentration on glucose release and ethanol yield during fermentation. (a) Effect of varying substrate concentrations (0.5, 1.0, 1.5, and 2.0%) on glucose release (mg mL^{-1}) over 72 h. (b) Corresponding ethanol yield (%) measured at different time intervals (12–72 h). Ethanol production increased steadily, reaching a maximum of 6.77% after 72 h, indicating efficient conversion of glucose into ethanol at optimal conditions.

Source: Author's contribution.

Table 4. Seeds for sustainable biodiesel and bioethanol production

Source	Sum of squares	df	Mean square	*F*-value	*p*-value	
Model	$3.545 \times 10^{+5}$	14	25319.56	78.65	<0.0001	Significant
A-temperature	$2.655 \times 10^{+5}$	1	$2.655 \times 10^{+5}$	824.65	<0.0001	
B-time	1226.37	1	1226.37	3.81	0.0699	
C-acid conc.	14299.02	1	14299.02	44.41	<0.0001	
D-subs. conc.	45.74	1	45.74	0.1421	0.7115	
AB	280.38	1	280.38	0.8709	0.3655	
AC	45.81	1	45.81	0.1423	0.7113	
AD	891.32	1	891.32	2.77	0.1169	
BC	3673.57	1	3673.57	11.41	0.0041	
BD	6855.05	1	6855.05	21.29	0.0003	
CD	1.70	1	1.70	0.0053	0.9431	
A^2	42696.64	1	42696.64	132.62	<0.0001	
B^2	11642.50	1	11642.50	36.16	<0.0001	
C^2	9683.89	1	9683.89	30.08	<0.0001	
D^2	2324.56	1	2324.56	7.22	0.0169	
Residual	4829.19	15	321.95			
Lack of fit	4816.85	10	481.68	195.10	<0.0001	Significant
Pure error	12.34	5	2.47			
Cor total	$3.593 \times 10^{+5}$	29				

Source: Author's contribution.

3.9 Response surface regression: Glucose conc. vs time, temperature, acid

The RSM model for glucose concentration was highly significant and demonstrated excellent predictive power. The model's ANOVA results (Table 4) showed a *p*-value of less than 0.0001, confirming high statistical significance.

The high R^2 value of 0.9741 indicates the model explains 97.41% of the variability in the data, confirming an excellent fit to the experimental results. This is further supported by an adjusted R^2 of 0.9379 and a predicted R^2 of 0.9004, which demonstrates robust predictive ability for new data (Table 5).

Analysis of the model coefficients (Table 6) revealed significant interactive effects between the process parameters, particularly between temperature and time

Table 5. Model Summary

S	*R*-sq	*R*-sq (adjusted)	*R*-sq (predicted)
17.94	R^2 = 98.66%	97.40%	93.70%

Source: Author's contribution.

Table 6. Regression Equation in Uncoded Units

Enzyme activity	=
+170.02	
+117.61	*A*
+7.61	*B*
−27.07	*C*
+1.49	*D*
+4.05	*AB*
−1.69	*AC*
+7.46	*AD*
−15.15	*BC*
−19.70	*BD*
−0.3256	*CD*
+71.42	A^2
−28.84	B^2
−24.23	C^2
−11.59	D^2

Source: Author's contribution.

Table 7. Glucose yield (mg mL^{-1}) during enzymatic hydrolysis

Time	6 h	24 h	48 h	72 h
Enzyme conc.	mg mL^{-1}	mg mL^{-1}	mg mL^{-1}	mg mL^{-1}
Control	80.01	80.02	80.04	80.04
0.5 mL	70.91	72.11	108.31	110.12
1.0 mL	74.01	84.32	110.21	112.24
1.5 mL	81.41	96.89	112.22	115.12
2.0 mL	85.11	104.01	116.19	118.21

Source: Author's contribution.

(p = 0.039). The model's high fitness (97.41%) aligns with previously validated studies, confirming the reliability of the regression model for optimization [18].

3.10 Enzymatic hydrolysis

To overcome the inherent recalcitrant nature of the pretreated *P. pinnata* biomass, due to the complex structure of cellulose and hemicelluloses in lignocellulosic biomass [53], enzymatic hydrolysis was employed to convert cellulose and hemicelluloses into fermentable sugars [54,55]. Enzymatic hydrolysis remains essential for converting recalcitrant hemicellulose and cellulose into fermentable monomers [56]. A 1:1 mixture of endoglucanase and exoglucanase at different doses (0.5, 1, 1.5, and 2 mL) was used, and its concentration and incubation time were optimized.

The maximum glucose yield of 118.21 mg g^{-1} was achieved using a 2.0-mL enzyme load and a 72-h incubation period (Figure 6a, Table 7). This result is consistent with the response surface model, where a contour plot indicated optimal glucose release within an enzyme concentration range of 1.5–2.0 U mL^{-1} and an incubation time of 50–70 h. These findings align with previous reports on the enzymatic conversion of lignocellulosic biomass into fermentable sugars. For instance, similar enzymatic treatments have yielded 50% glucose recovery from rice hulls [41] and 80% total glucose yield from wheat bran after, followed by a 5% enzymatic load for 72 h [41]. The effectiveness of enzyme cocktails (cellulase, xylanase, hemicellulase, and glucosidase) for enhancing sugar yields is well-established, further validating the approach used here [57]. Similarly, our results for *P. pinnata* (429 mg g^{-1} glucose) compare favorably with the yields obtained from rice polish, which we previously achieved, where enzymatic hydrolysis was also found to be a necessary secondary step to achieve industrial-scale sugar concentrations [58,59]. The RSM model demonstrated high reliability (R^2 = 0.9741), reflecting the exploitation of RSM in optimizing bioethanol production from other non-edible feedstocks like *Bombax ceiba* [60].

3.11 Fermentation of *P. pinnata*

Following optimization of all physiochemical parameters, acidic pretreatment, and enzymatic saccharification of *P. pinnata*, fermentation was conducted using *S. cerevisiae*. This yeast was selected for its industrial prominence, owing to its efficient sugar metabolism, high ethanol yield, and environmental robustness [61].

Fermentation was conducted with 40 g of pretreated *P. pinnata* biomass under optimal conditions using a 3 mL inoculum containing 1 × 10^7 cells mL^{-1} of *S. cerevisiae* at 37°C. Ethanol production was monitored at different time-intervals: 6, 24, 48, and 72 h. The maximum ethanol production of 6.71% was observed at 72 h and then declined (Figure 6b). The subsequent decline in ethanol concentration is likely due to the depletion of sugars and the yeast shifting to maintenance metabolism. Our findings align with previous studies that have demonstrated optimal fermentation conditions for various microorganisms. Nimbkar *et al.* [62] reported maximum ethanol production (12.45%) from unsterilized sweet sorghum juice at 30°C. Similarly, Chongkhong [63] and Iqbal *et al.* [18] observed a positive correlation between ethanol yield and increasing pH (4.4–5.9) and temperature (27–36°C), although a decline in yield was noted at higher values. Furthermore, *Pichia stipitis* BCC15191 yielded high ethanol concentrations from bagasse hydrolysate at 30°C and pH 5.5 after 72 h of incubation [64]. However, our results differed from those obtained by Markou et al. (56% yield with *Arthrosphira platensis*) and Ho *et al.* (90% yield with *Chlorella vulgaris* [65]. These discrepancies can be attributed to variations in the microorganisms used and their specific growth requirements.

4. Conclusions

This study confirmed the potential of *P. pinnata* seeds as a versatile and sustainable feedstock for integrated biofuel production. The seeds exhibited favorable physicochemical properties, and FTIR analysis confirmed a lignocellulosic composition conducive to efficient biomass deconstruction. Biodiesel production via transesterification of the seed oil yielded up to 70% biodiesel at an optimal alcohol-to-oil ratio of 5:1. Statistical optimization using

RSM effectively identified pretreatment conditions that maximized glucose release (429 mg g^{-1}), highlighting the critical roles of temperature, acid concentration, substrate loading, and incubation time in overcoming biomass recalcitrance. Subsequent enzymatic hydrolysis further improved fermentable sugar availability, while fermentation with *S. cerevisiae* yielded a maximum ethanol of 6.71% at 72 h. Collectively, these findings highlighted the dual potential of *P. pinnata* for biodiesel and bioethanol production, offering a promising strategy for renewable energy generation and reduced dependence on fossil fuels. Future work should focus on techno-economic analysis, pilot-scale production, inhibitor mitigation, and exploring co-product valorization to yield sustainable and economic viability of the *P. pinnata* integrated biorefinery.

Acknowledgments

The authors are thankful to the lab support staff (University of Gujrat, Pakistan) for their help during the course of this study.

Author contributions

Conceptualization, Z.A. and Z.I.; Investigation, S.R.; methodology, S.R., Z.A. and Z.I.; writing – original draft preparation, S.R, Z.I. and Z.A.; writing – review and editing, Z.I., H.M.J., A.G., and Z.A. All authors have read and agreed to the published version of the manuscript.

Funding information

The authors extend their gratitude to the Deanship of Scientific Research, Vice Presidency for Graduate Studies and Scientific Research, King Faisal University, Kingdom of Saudi Arabia, for funding the publication of this work (Grant KFU260717).

Conflicts of interest statement

The authors declare no conflicts of interest.

Data availability statement

All the data related to this study are presented in the main script and in Supplementary data.

References

[1] Sandesh, K., Ujwal, P., Trends and perspectives of liquid biofuel–Process and industrial viability, Energy Convers. Manag., 2021; 10(1): 100075. doi: 10.1016/j.ecmx.2020.100075

[2] Tripathi, C., Baredar, P., Tripathi, L., Air pollution in Delhi: Biomass energy and suitable environmental policies are sustainable pathways for health safety, Curr. Sci., 2019; 117(7): 1153–1160. doi: 10.18520/cs/v117/i7/1153-1160

[3] Zou, J., Chang, X., Past, present, and future perspectives on whey as a promising feedstock for bioethanol production by yeast, J. Fungi., 2022; 8(4): 395. doi: 10.3390/jof8040395

[4] Bekele B.A., Abdissa Akuma, D., Hundie, B.K., An integrated approach to optimization of fermentation conditions for bioethanol production from local left-over Injera waste using central composite design, Environ. Health Eng. Manag. J., 2022; 9(4): 281–293. doi: 10.34172/EHEM.2022.29

[5] Broda, M., Yelle, D.J. Serwańska, K., Bioethanol production from lignocellulosic biomass – challenges and solutions, Molecules, 2022; 27(24): 8717. doi: 10.3390/molecules27248717

[6] Scully, S.M., Orlygsson, J., Recent advances in second-generation ethanol production by thermophilic bacteria, Energies, 2014; 8(1): 1–30. doi: 10.3390/en8010001

[7] Wang, L., Liu, S., Mehdi, S., Liu, Y., Zhang, H., Shen, R., et al., Lignocellulose-derived energy materials and chemicals: A review on synthesis pathways and machine learning applications, Small Methods, 2025; 9(8): e2500372. doi: 10.1002/smtd.202500372

[8] Anwar, F., Tariq, M., Nisar, J., Ali, G., Kanwal, H., Optimization of biodiesel yield from non-food karanja seed oil: Characterization and assessment of fuel properties, Sustain. Chem. Environ., 202; 3(1): 100035. doi: 10.1016/j.scenv.2023.100035

[9] Devidas, T.B., Vyas, A., Sridhar, K., Chawla, P., Bains, A., Sharma, M., Valorization of pongame oil tree (*Millettia pinnata*) seed and seed oil: A promising source of phytochemicals and its applications, Waste Biomass Valor., 2024; 15(9): 5705–5717. doi: 10.1007/s12649-023-02352-9

[10] Meher, L.C., Dharmagadda, V.S.S., Naik, S.N., Optimization of alkali-catalyzed transesterification of Pongamia pinnata oil for biodiesel production, Bioresour. Technol., 2006; 97(12): 1392–1397. doi: 10.1016/j.biortech.2005.07.003

[11] Jeelani, I., Qadir, T., Sheikh, A., Bhosale, M., Sharma, P.K., Amin, M.A., et al., *Pongamia pinnata*: An heirloom herbal medicine, Open Med. Chem. J., 2023; 17(1): e18741045240484. doi: 10.2174/0118741045240484231009141434

[12] Akram, M., Nimesh, S., Chishti, M.A., Ahmad, M.A., Dhama, S., Lal, M., *Pongamia pinnata*: An updated review on its phytochemistry and pharmacological uses, Pharm. Pharmacol. Int. J., 2021; 9(5): 194–199. doi: 10.15406/ppij.2021.09.00344

[13] Nikolić, B.D., Markovic, N.S., Petrovic, N.S., Markinkovic, D.Z., Jovanovic, V.D., Biodiesel and feedstocks – possibilities and characteristics: A review, Therm. Sci., 2025; 29(1): 58–68. doi: 10.2298/TSCI250205058N

[14] Soares, J.F., Confortin, T.C., Todero, I., Luft, L., Ugalde, G.U., Tovar, L.P., et al., Estimation of bioethanol, biohydrogen, and chemicals production from biomass wastes in Brazil, Clean Soil Air Water, 2022; 50(12): 2200155. doi: 10.1002/clen.202200155

[15] Ali, M., Sultana, R., Tahir, S., Watson, I.A., Saleem, M., Prospects of microalgal biodiesel production in Pakistan – a review, Renew. Sustain. Energy Rev., 2017; 80(1): 1588–1596. doi: 10.1016/j.rser.2017.08.062

[16] Mishra, P., Girdoniya, V., Biofuels: Alternative resources of energy, Academic Press. San Diego, California, USA. 2018

[17] El-Fawal, E.M., El Naggar, A.M.A., El-Zahhar, A.A., Alghandi, M.M., Morshedy, A.S., El Sayeda, H.A., et al., Biofuel production from waste residuals: Insights into biomass conversion technologies and engineered biochar applications, RSC Adv., 2025; 15(18): 11942–11974. doi: 10.1039/d5ra00857c

[18] Iqbal, Z., Siddiqua, A., Anwar, Z. Munir, M., Valorization of *Delonix regia* pods for bioethanol production, Fermentation, 2023; 9(3): 289. doi: 10.3390/fermentation9030289

[19] Riffat, A., Anwar, Z., Zafar, M., NAdeem, F., Mehmood, T., Optimization and characterization of laccase produced by Fomes fomentarius through solid-state fermentation, Biomass Convers. Biorefin., 2024; 14(3): 3999–4006. doi: 10.1007/s13399-022-02621-y

[20] Suresh, R., Ashwin, R. MohanRaj, T., Experimental investigation of LHR engine performance using *Pongamia pinnata* and *Azadirachta indica* biodiesel blends, SAE Tech. Pap., 2025; 5(2): 0148–7191. doi: 10.4271/2025-28-0039

[21] Patel, A., Shah, R., Mehta, P., Environmental considerations in solvent extraction methods for oil extraction, Green Chem. Rev., 2019; 15(2): 120–135

[22] Dandash, A.A., Abu-Jdayil, B., Tannous, J.H., Lignin extraction from various biomass sources: Characteristics, applications, and future prospects, Chem. Rec., 2025; 25(1): e2500045. doi: 10.1002/tcr.202500045

[23] Husaini, S., Kadire, A., Verma, R.K., Pydimalla, M., Biodiesel production from non-edible mixed oils: A sustainable approach using jatropha, karanja and waste cooking oil, Bull. Mater. Sci., 2025; 48(2): 58. doi: 10.1007/s12034-025-03414-5

[24] Tang, Y., Zhang, H., Liu, Z., Wang, X., Li, Y., Multi-objective optimization of methanol reforming reactor performance using response surface methodology and particle swarm optimization, Energy Convers. Manag., 2024; 307(1): 118377. doi: 10.1016/j.enconman.2024.118377

[25] Olia, M.S.J., Azin, M., Moazami, N., Comparison of pretreatment methods for carbohydrate release from microalgae: A critical step in bioethanol production, Biomass Convers. Biorefin., 2022; 13(18): 17119–17132. doi: 10.1007/s13399-022-02426-z

[26] Sahu, T., Choudhary, R., Kulkarni, P., Isolation and screening of cellulase-producing bacteria from sugar industry waste, Res. J. Agric. Sci., 2024; 15(3): 918–921

[27] Mtashobya, L.A., Mgeni, S.T., Emmanuel, J.K., Bioethanol production from concentrated fruit waste juice using bakery yeast, Mater. Renew. Sustain. Energy, 2025; 14(1): 6. doi: 10.1007/s40243-024-00283-6

[28] Abdulrahman, M., Bioethanol production from selected agro-wastes using *Saccharomyces cerevisiae* strain CBS 1171 and *Lactobacillus delbrueckii* strain MN945906, M. Tech thesis, Federal University of technology, Minna, Nigeria; 2021

[29] Bennett, C., Spectrophotometric acid dichromate method for the determination of ethyl alcohol, Am. J. Med. Technol., 1971; 37(6): 217–220

[30] Cahyono, D.D.N., Hidayat, W., Riniarti, M., Bintoro, A., Effects of storage-induced moisture loss on germination performance and oil yield of *Pongamia pinnata*, J. Sylva Lestari, 2025; 13(1): 145–158. doi: 10.23960/jsl.v13i1.1026

[31] Deswal, R., Kaushik, N., Panwar, N., Rawat, L., Bangarwa, K., Seed viability and oil content of *Pongamia pinnata* stored under different moisture and temperature regimes, Res. Crops, 2015; 16(3): 568–578. doi: 10.5958/2348-7542.2015.00081.9

[32] Sahu, B., Sahu, A.K., Thomas, V., Naithani, S.C., Oxidative stress, lipid peroxidation and antioxidative enzymes in dehydrating *Pongamia pinnata* seeds during storage, S. Afr. J. Bot., 2017; 112(1): 383–390. doi: 10.1016/j.sajb.2017.06.030

[33] Peters, F.B., Rapp, A.O., Moisture as a key factor in understanding lignocellulose fluorescence in wood, Cellulose, 2024; 31(7): 4149–4160. doi: 10.1007/s10570-024-05898-6

[34] Ingle, A.P., Chandel, A.K., Philippini, R.R., Rai, M., Sustainable production of biomaterials and biochemicals from lignocellulosic biomass, Biotechnol. Sustain. Mater., 2025; 2(1): 3. doi: 10.1186/s44316-025-00025-2

[35] Zhuang, J., Li, M., Pu, Y., Ragauskas, A.J., Yoo, C.G., Observation of potential contaminants in processed biomass using Fourier transform infrared spectroscopy, Appl. Sci., 2020; 10(12): 4345. doi: 10.3390/app10124345

[36] Boukir, A., Fellak, S., Doumenq, P., Structural characterization of Moroccan wooden artifacts during natural degradation using ATR-FTIR and XRD, Heliyon, 2019; 5(9): e01545. doi: 10.1016/j.heliyon.2019.e02477

[37] Smith, B., The infrared spectroscopy of alkenes, Spectroscopy, 2016; 31(11): 30–33

[38] Awoyale, A.A., Lokhat, D., Effects of pretreatment on selected Nigerian lignocellulosic biomass for bioethanol production, Sci. Rep., 2021; 11(1): 557. doi: 10.1038/s41598-020-78105-8

[39] Irfan, M., Syed, Q., Abbas, S., GulSher, M., Baig, S., Nadeem, M., FTIR and SEM analysis of thermochemically fractionated sugarcane bagasse, Turk. J. Biochem., 2011; 36(4): 322–328

[40] Gaur, A., Mishra, S., Chowdhury, S., Baredar, P., Verma, P., Factors affecting biodiesel production from waste cooking oil: An Indian perspective, Mater. Today Proc., 2021; 46(13): 5594–5600. doi: 10.1016/j.matpr.2020.09.432

[41] Maweekubure Gedara, S.S.B., Process design and simulation for biodiesel production. MSc thesis, Faculty of Technology, Natural sciences and Maritime Sciences, University of South-Eastern, Norway; 2025

[42] Meng, X., Chen, G., Wang, Y., Biodiesel production from waste cooking oil via alkali catalysis and engine testing, Fuel Process. Technol., 2008; 89(9); 851–857. doi: 10.1016/j.fuproc.2008.02.006

[43] Ewunie, G.A., Morken, J., Lekang, O.I., Yigezu, Z.D., Factors affecting the potential of *Jatropha curcas* for sustainable biodiesel production, Renew. Sustain. Energy Rev., 2021; 137(1): 110500. doi: 10.1016/j.rser.2020.110500

[44] Sharma, H.K., Xu, C., Qin, W., Biological pretreatment of lignocellulosic biomass for biofuels and bioproducts, Waste Biomass Valor., 2019; 10(1): 235–251. doi: 10.1007/s12649-017-0059-y

[45] Hussein, Z.E.H., Silva, J.M., Castro, M.C., Borges, N.E., Saqueti, B.H.F., Optimization of almond beverage enriched with omega-3 fatty acids using D-optimal mixing design, Food Technol. Biotechnol., 2025; 63(2): 274–284. doi: 10.17113/ftb.63.02.25.8460

[46] Li, M.-F., Introduction to pretreatment for biofuel production, In Pretreatment of lignocellulosic biomass for bioenergy production, Woodhead Publishing, Canbridge, United Kingdom; 2026. pp. 1–14. doi: 10.1016/B978-0-443-24714-9.00003-4

[47] Selvakumar, P., Vimal, J., Kavitha, S., Preethi, R., Rajesh, R., Optimization of binary acid pretreatment of corncob biomass for enhanced cellulose recovery, Fuel, 2022; 321(1): 124060. doi: 10.1016/j.fuel.2022.124060

[48] Awoyale, A.A., Lokhat, D., Hybridization of Nigerian lignocellulosic biomass for bioethanol production: Modeling and optimization, J. Oleo Sci., 2021; 70(7): 1013–1026. doi: 10.5650/jos.ess21038

[49] Kahlouche, F.Z., Zerrouki, S., Bouhelassa, M., Rihani, R., Optimization of enzymatic and thermochemical pretreatment of bread waste for bioethanol production, Water Sci. Technol., 2022; 85(12): 3436–3450. doi: 10.2166/wst.2022.190

[50] Kim, J.-W., Kim, K.-S., Lee, J.-S., Park, S.-M., Lee, J.-C., Two-stage pretreatment of rice straw using aqueous ammonia and dilute acid, Bioresour. Technol., 2011; 102(17): 8992–8999. doi: 10.1016/j.biortech.2011.06.068

[51] Tang, J., Chen, K., Huang, F., Li, J., Characterization of pretreatment liquor from *Eulaliopsis binata* for dissolving pulp production, Bioresour. Technol., 2013; 129(1): 548–552. doi: 10.1016/j.biortech.2012.11.096

[52] Bondesson, P.-M., Galbe, M., Zacchi, G., Ethanol and biogas production after steam pretreatment of corn stover with or without sulfuric acid, Biotechnol. Biofuels, 2013; 6(1): 11. doi: 10.1186/1754-6834-6-11

[53] Kassim, M.A., Meng, T.K., Kamaludin, R., Hussain, A.H., Bukhari, N.A., Biofuel value-chain development, In Value-chain of biofuels, Elsevier, Amsterdam, The Netherlands; 2022. pp. 195–234. doi: 10.1016/B978-0-12-824388-6.00004-X

[54] Vasić, K., Knez, Ž., Bioethanol production by enzymatic hydrolysis from different lignocellulosic sources, Molecules, 2021; 26(3): 753. doi: 10.3390/molecules26030753

[55] Gao, J., Anderson, D., Levie, B., Saccharification of recalcitrant biomass and integration options for lignocellulosic sugars, Biotechnol. Biofuels, 2013; 6(1): 10. doi: 10.1186/1754-6834-6-10

[56] de Carvalho, M.S., de Menezes, L.H.S., Pimentel, A.B., Costa, F.S., Oliveira, P.C., de Santos, M.M.O., et al.,

Chemometric optimization of xylanase secretion and its application in saccharification of agro-industrial waste, Waste Biomass Valor. 2023; 14(9): 3183–3193. doi: 10.1007/s12649-022-01832-8

[57] de Azevedo Seara, M.F.M., Sustainable production of postbiotics for food applications, MSc thesis, Universidade Católica Portuguesa; 2023; Palma de Cima, 1649-023 Lisboa, Portugal

[58] Anwar, Z., Gulfraz, M., Imran, M., Asad, M.J., Al-Shafi, A., Anwar, P., et al., Optimization of dilute acid pretreatment for bioethanol production from rice polish, Pak. J. Bot., 2012; 44(1): 169–176. doi: 10.5897/AJB11.1145

[59] Anwar, Z., Gulfraz, M., Asad, M.J., Imran, M., Akram, Z., Mehmood, S., et al., Bioethanol production from rice polish by optimized pretreatment and enzymatic hydrolysis, Afr. J. Biotechnol., 2012; 11(4): 992–998. doi: 10.5897/AJB11.1145

[60] Ghazanfar, M., Irfan, M., Nadeem, M., Shakir, H.A., Khan, M., Ahmad, I., et al., Optimization of bioethanol production from KOH-pretreated *Bombax ceiba* using *Saccharomyces cerevisiae*, Fermentation, 2022; 8(4): 148. doi: 10.3390/fermentation8040148

[61] Walker, G.M., Stewart, G.G., Enhancing yeast alcoholic fermentations, Adv. Appl. Microbiol., 2018; 105(1): 87–129. doi: 10.1016/bs.aambs.2018.05.003

[62] Nimbkar, N., Ghanekar, A., Joseph, R., Development of improved sweet sorghum cultivars for ethanol production, In Ingle, U.M., Kulkarni, D.N., Thorat, S.S., eds. Technology and application for alternative uses of sorghum, Proceedings of the National Seminar held on Feb. 2–3, 1987 at Marathwada Agricultural University, Parbhani; 1987

[63] Chongkhong, S., Response surface optimization of ethanol production from banana peels by organic acid hydrolysis and fermentation, Songklanakarin J. Sci. Technol., 2017; 39(1): 1–9. doi: 10.14456/sjst-psu.2017.28

[64] Buaban, B., Inoue, H., Yano, S., Tanapongpipat, S., Ruanglek, V., Champreda, V., et al., Bioethanol production from ball-milled bagasse using on-site produced fungal enzyme cocktail, Biotechnol. Biofuels, 2012; 5(1): 1–10. doi: 10.1016/j.jbiosc.2009.12.003

[65] Markou, G., Angelidaki, I., Nerantzis, E., Georgakakis, D., Bioethanol production by carbohydrate-enriched biomass of *Arthrospira (Spirulina) platensis*, Energies, 2013; 6(8): 3937–3950. doi: 10.3390/en6083937